

## Comparative transcriptome analysis of papilla and skin in the sea cucumber, *Apostichopus japonicus*

Xiaoxu Zhou, Jun Cui, Shikai Liu, Derong Kong, He Sun, Chenlei Gu, Hongdi Wang, Xuemei Qiu, Yaqing Chang, Zhanjiang Liu, Xiuli Wang

Papilla and skin are two important organs of the sea cucumber. Both tissues have ectodermic origin, but they are morphologically and functionally very different. In the present study, we performed comparative transcriptome analysis of the papilla and skin from the sea cucumber (*Apostichopus japonicus*) in order to identify and characterize gene expression profiles by using RNA-Seq technology. We generated 30.6 and 36.4 million clean reads from the papilla and skin and *de novo* assembled in 156,501 transcripts. The gene ontology (GO) analysis indicated that cell part, metabolic process and catalytic activity were the most abundant GO category in cell component, biological process and molecular function, respectively. Comparative transcriptome analysis between the papilla and skin allowed the identification of 1,059 differentially expressed genes, of which 739 genes were expressed at higher levels in papilla, while 320 were expressed at higher levels in skin. In addition, 236 differentially expressed unigenes were not annotated with any database, 160 of which were apparently expressed at higher levels in papilla, 76 were expressed at higher levels in skin. We identified a total of 288 papilla-specific genes, 171 skin-specific genes and 600 co-expressed genes. And 40 genes in papilla-specific were not annotated with any database, 2 in skin-specific. Development-related genes were also enriched, such as *fibroblast growth factor*, *transforming growth factor- $\beta$* , *collagen- $\alpha$ 2* and *Integrin- $\alpha$ 2*, which may be related to the formation of the papilla and skin in sea cucumber. Further pathway analysis identified ten KEGG pathways that were differently enriched between the papilla and skin. The findings on expression profiles between two key organs of the sea cucumber should be valuable to reveal molecular mechanisms involved in the development of organs that are related but with morphological differences in the sea cucumber.

1 **Comparative transcriptome analysis of papilla and skin in the sea cucumber,**

2 *Apostichopus japonicus*

3 **Xiaoxu Zhou<sup>1,2\*</sup>, Jun Cui<sup>2\*</sup>, Shikai Liu<sup>3\*</sup>, Derong Kong<sup>2</sup>, He Sun<sup>2</sup>, Chenlei Gu<sup>2</sup>, Hongdi**  
4 **Wang<sup>2</sup>, Xuemei Qiu<sup>1,2</sup>, Yaqing Chang<sup>1,2</sup>, Zhanjiang Liu<sup>3</sup>, Xiuli Wang<sup>1,2</sup>**

5

6 <sup>1</sup> Key Laboratory of Mariculture&Stock Enhancement in North China's Sea, Ministry of  
7 Agriculture, Dalian Ocean University, Dalian, 116023, China.

8 <sup>2</sup> College of Fisheries and Life Science, Dalian Ocean University, 52 Heishijiao Street,  
9 Shahekou District, Dalian, 116023, China.

10 <sup>3</sup> The Fish Molecular Genetics and Biotechnology Laboratory, Aquatic Genomics  
11 Unit, School of Fisheries, Aquaculture and Aquatic Sciences and Program of Cell and  
12 Molecular Biosciences, Auburn University, Auburn, AL 36849, USA.

13

14 \* These authors contributed equally to this work.

15

16 Corresponding Author:

17 Xiuli Wang

18 Address: 52, Heishijiao Street, Shahekou District, Dalian, Liaoning 116023, China.

19 E-mail: xiuliwang417@sina.com.

20 Tel.: +86-411-84763589

21

22

23

24

25

26

27

**28 ABSTRACT**

29 Papilla and skin are two important organs of the sea cucumber. Both tissues have  
30 ectodermic origin, but they are morphologically and functionally very different. In the present  
31 study, we performed comparative transcriptome analysis of the papilla and skin from the sea  
32 cucumber (*Apostichopus japonicus*) in order to identify and characterize gene expression profiles  
33 by using RNA-Seq technology. We generated 30.6 and 36.4 million clean reads from the papilla  
34 and skin and *de novo* assembled in 156,501 transcripts. The gene ontology (GO) analysis  
35 indicated that cell part, metabolic process and catalytic activity were the most abundant GO  
36 category in cell component, biological process and molecular function, respectively.  
37 Comparative transcriptome analysis between the papilla and skin allowed the identification of  
38 1,059 differentially expressed genes, of which 739 genes were expressed at higher levels in  
39 papilla, while 320 were expressed at higher levels in skin. In addition, 236 differentially  
40 expressed unigenes were not annotated with any database, 160 of which were apparently  
41 expressed at higher levels in papilla, 76 were expressed at higher levels in skin. We identified a  
42 total of 288 papilla-specific genes, 171 skin-specific genes and 600 co-expressed genes. And 40  
43 genes in papilla-specific were not annotated with any database, 2 in skin-specific. Development-  
44 related genes were also enriched, such as *fibroblast growth factor*, *transforming growth factor-*  
45  *$\beta$* , *collagen-  $\alpha$  2* and *Integrin-  $\alpha$  2*, which may be related to the formation of the papilla and skin  
46 in sea cucumber. Further pathway analysis identified ten KEGG pathways that were differently  
47 enriched between the papilla and skin. The findings on expression profiles between two key  
48 organs of the sea cucumber should be valuable to reveal molecular mechanisms involved in the  
49 development of organs that are related but with morphological differences in the sea cucumber.

**50 KEYWORDS**

51 Comparative transcriptome, Skin, Gene expression, High-throughput sequencing, Papilla, Sea

52 cucumber (*Apostichopus japonicus*)

### 53 INTRODUCTION

54 Sea cucumbers group (Echinodermata, Holothuroidea) comprise of approximately 1,250  
55 species (Du et al. 2012). Sea cucumbers are mostly processed into a dry product called trepang,  
56 bêche-de-mer or hai-san, which is widely recognized as a delicate food with medicinal effect for  
57 human consumption. Sea cucumbers have been harvested commercial use since a thousand years  
58 ago, and they are now widely cultured in more than 70 countries (Steven, Purcell & Chantal,  
59 2012). The sea cucumber *Apostichopus japonicus* (Holothuroidea, Aspidochirotida) is  
60 intensively cultured in many East Asian countries and is naturally found along the coasts of  
61 China, Japan, Korea and Russia of Northeast Asia (Sloan, 1984; Chang et al., 2009). It is  
62 intensively cultured as an important aquaculture species in many countries of East Asia.

63 The pentamerous radial symmetry is considered as one of the characteristics of  
64 echinodermata. In sea cucumber, pentamerous symmetry is usually determined based on the  
65 presence of five meridional ambulacra bearing podia (Steven, Purcell & Chantal, 2012). Papillae  
66 represent the podia on the dorsal surface, and generally have no locomotive function. With *A.*  
67 *japonicus*, fleshy and conical papillae, with a sensory spina at its apex, are present in two loose  
68 rows on the dorsal surface and two rows at the lateral margins of the ventral surface (Steven,  
69 Purcell & Chantal, 2012). Previous studies have investigated the morphological characteristics of  
70 papilla in the *A. japonicus* (Vanden et al., 1995; Chang et al., 2011; Steven, Purcell & Chantal,  
71 2012). In the papillae, the ciliated cells and histamine-like immunoreactivity neurons are in  
72 contact with the nerve plexus (Hyman, 1955; Luke et al., 2012). Therefore, the dorsal papillae  
73 have long been associated to a sensory role, which may involve chemoreception and  
74 mechanoreception (Vanden et al., 1995).

75 The thicker body wall of *A. japonicus* consists of a thin cuticle over the epidermis and a  
76 thick dermis underneath. The cuticle and epidermis as the outer tissues of the *A. japonicus* are  
77 represented by skin (Steven, Purcell & Chantal, 2012). The skin forms a protective barrier,  
78 forming the first line of defence against the environment. Previous studies have been conducted

79 on skin with main focused on the intrinsic mechanisms underlying immune response to skin  
80 ulceration and peristome tumescence (Liu et al., 2010; Zhang et al., 2013).

81 The papillae are closely associated with the skin in sea cucumber. Both organs are mainly  
82 composed of collagen (up to 70%), and are the major component of the body wall. Moreover, the  
83 papillae and skin are formed by similar elements and homologous cell types, such as  
84 keratinocytes, epidermis and dermis, all derived from the ectoderm (Chang et al., 2004; Lowdon  
85 et al., 2014). Despite the common embryonic origin of the two organs, they exhibit clear  
86 morphological differences and play distinct functions. The molecular mechanisms underlying  
87 differentiation between the papilla and skin remain largely unknown. The lack of reference  
88 genome and the limited genetic resources of *A. japonicus* represent a major obstacle to better  
89 understand the function of these two organs.

90 In this study, we conducted RNA-Seq of these two organs to determine global changes in  
91 gene expression between the papilla and skin in the *A. japonicus*. RNA-Seq technology has been  
92 widely used for the generation of genetic resources in echinoderms (Anisimov, 2008; Wang,  
93 Gerstein & Snyder, 2009). Recently, several RNA-Seq based transcriptome analyses have been  
94 conducted in the *A. japonicus*, including studies on histology (Sun et al., 2011, 2013),  
95 immunology (Li et al., 2012), physiology (Zhao et al., 2014a, 2014b), embryonic development  
96 and gene marker discovery (Du et al. 2012; Zhou et al. 2014). The first transcriptome sequencing  
97 of the *A. japonicus* intestine and body wall was performed by Sun et al (Sun et al., 2011).  
98 Thereafter, the global dynamic changes during all stages of intestine regeneration were further  
99 investigated (Sun et al., 2013). To identify candidate transcripts potentially involved in  
100 aestivation and generate a wide coverage of transcripts involved in a broad range of biological  
101 processes, eight cDNA libraries were constructed and sequenced by Du et al. (Du et al., 2012).  
102 Immune-related genes and pathways in response to pathogen infection were identified (Zhou et  
103 al., 2014; Gao et al., 2015). Moreover, many physiological networks were identified and  
104 characterized in the *A. japonicus* on the basis of transcriptomic resources (Wang et al., 2015;  
105 Yang et al., 2015).

106 Here, in this work, we report comparative transcriptome analysis of the papilla and skin. A  
107 relatively large number of genes that displayed distinct expression profiles between the papillae  
108 and skin were identified. Further enrichment analysis identified pathways such as tight junction  
109 and p53 signaling pathway could be involved in the development of the papilla and skin. This  
110 work provided the essential genomic resources for further investigations into the molecular  
111 interactions and multiple biological process of appendages such as the papilla and skin in the *A.*  
112 *japonicus*.

## 113 MATERIALS AND METHODS

### 114 Sample collection

115 A total of 45 sea cucumbers (average weight of 25g) provided by the Key Laboratory of  
116 Mariculture in North China (Dalian, Liaoning) were used in the present study. In order to have a  
117 good reference transcriptome, the skin around the papillae, papilla and tube foot tissues were  
118 collected for RNA-Seq. We randomly group these 45 sea cucumbers into three groups as  
119 replicates. Within each group, ~1g tissue was dissected from each individual, respectively.  
120 Tissues collected from each group were of every individual were pooled (one pool per tissue)  
121 and placed in 2ml of RNeasy Lysis Solution (Qiagen) for overnight at 4°C followed by transferring  
122 to -80°C until RNA extraction.

### 123 RNA-Seq

124 Total RNA was extracted from the pooled samples using the TRIzol Reagent (Invitrogen,  
125 CA, USA) following the manufacturer's recommendations. The quantity and integrity of total  
126 RNA were assessed using an Agilent 2100 Bioanalyzer and 1% agarose gel electrophoresis. High  
127 quality RNA was used for the construction of cDNA. Library construction and sequencing was  
128 performed in the Biomarker Biotechnology Corporation (Beijing, China). Paired-end sequencing  
129 was conducted on an Illumina HiSeq 2500 platform to generate 125bp paired-end (PE) reads.

### 130 Transcriptome assembly and annotation

131 Low quality reads and adaptors were trimmed before assembly. Trimmed reads were *de novo*  
132 assembled by Trinity software using default parameters (Grabherr et al., 2011) and used as a

133 reference for gene expression analysis. Transcriptome was annotated using Basic Local  
134 Alignment Search Tool (BLAST) searches against the NCBI non-redundant (NR) database,  
135 Swiss-Prot, KEGG (the Kyoto Encyclopedia of Genes and Genomes) and GO (Gene ontology),  
136 Clusters of Orthologous Groups (COG) and eukaryotic Orthologous Groups (KOG) with e-value  
137 cutoff of  $1e^{-5}$ .

### 138 **Differentially Expressed Gene (DEG) Analysis**

139 Gene expression was determined by the FPKM (Fragments Per kb of transcript per Million  
140 mapped fragments) method. The gene expression differences between the papilla and skin tissues  
141 were identified following the formula:

$$142 \text{ Fold change} = \text{Log}_2 \frac{FPKM_{\text{Papilla}}}{FPKM_{\text{Skin}}}$$

143 DEGs were determined with the absolute fold change values greater than 2.0, and FDR  
144 (false discovery rate) lesser than 0.01 (Cui et al. 2014, 2015).

145 To further investigate DEGs identified between papilla and skin, genes were compared to  
146 those identified from the *A. japonicus* intestine RNA-Seq dataset (accession NO. GSE44995)  
147 from a previous study by Sun et al. (2013). Intestine is responsible for the metabolic rate  
148 depression under deep aestivating conditions (Chen et al., 2013) and play a role for organ  
149 regeneration (Sun et al., 2013). In the present study, we used intestine as major site in the  
150 internal environment of *A. japonicus* for further investigate DEGs identified between papilla and  
151 skin. All assembled sequences of *A. japonicus* published in Sun et al. (Sun et al., 2013) were  
152 downloaded as database to blast the DEGs, the differential expression of DEGs among the  
153 papilla, skin, and intestine was estimated using the formula:

$$154 \text{ Score} = \text{Log}_2 \frac{FPKM_{\text{Tissues}}}{RPKM_{\text{Intestines}}}$$

155 Where  $FPKM_{\text{Tissues}}$  indicates the FPKM of papilla or skin;  $RPKM_{\text{Intestines}}$  indicates the  
156 RPKM of intestine. Significant candidates were determined as the absolute score greater than 4.0.

### 157 **qRT-PCR validation**

158 RNA-Seq results were validated by qRT-PCR analysis of 16 randomly selected DEGs.  
159 Primers were designed following the manufacturer's recommendations of SYBR Premix Ex  
160 Taq™ II kit (Takara, Dalian). The  $\beta$ -actin was used as housekeeping. All the primers are  
161 shown in supplementary TableS1. Briefly, the amplification was performed in a total volume of  
162 16  $\mu$ L, containing 8 $\mu$ L 2 $\times$  SYBR Premix Ex Taq II, 1 $\mu$ L of cDNA, and 0.3 $\mu$ L of 10 $\mu$ M of each  
163 gene-specific primer. The qRT-PCR reactions were performed on ABI stepone plus platform and  
164 replicated in three pools. And three technical replications were performed for each qRT-PCR  
165 validation. PCR was conducted as follows: 94 °C for 30 s, 45 cycles of 94 °C for 5s, annealing  
166 temperature (showed in TableS1 ) for 15s, and 72 °C for 15s.

#### 167 **Gene enrichment analysis**

168 The gene enrichment analysis was conducted using KEGG database. The over-presentation  
169 of the DEGs was determined in the specific pathways. The level of enrichment was indicated by  
170 enrichment factor, and p-value was used to calculate the significance of enrichment. The top 10  
171 KEGG enrichments were selected to carry out further analysis.

## 172 **RESULTS**

### 173 **Sample sequencing**

174 RNA-Seq of the papilla and skin samples yielded over 70 million pair-end reads with  
175 average length of 125bp (Table 1). Similar number of reads was obtained from both tissues, with  
176 over 33 million reads from papilla and over 37 million from skin. After trimming, 30.6 and 36.4  
177 million high-quality reads were retained from papilla and skin, respectively. Totally, 7.7 billion  
178 bases generated from the papilla, 9.2 billion bases generated for the skin and 8.6 billion bases  
179 generated for the tube foot were used for down-stream analysis of *de novo* assembly and  
180 mapping. Data obtained from papilla, skin and tube foot were deposited to the sequence read  
181 archive (SRA) with the accession numbers of SRA275705 and SRA275706.

### 182 **Transcriptome assembly and annotation**

183 The *de novo* assembly resulted in a total of 156,501 transcripts, with the average length of

184 910.77bp and N50 length of 1,694bp (Table 2). The length distribution of transcripts and  
185 unigenes are shown in Fig. 1. Over 84% of reads from both tissues were successfully mapped  
186 back to the *de novo* transcriptome assembly.

187 The transcriptome assembly was annotated by BLASTX against NCBI NR, Pfam, Swiss-  
188 Prot, KEGG, COG and KOG databases with E-value threshold of  $1e-5$ . Annotation resulted in  
189 the identification of 92,343 unigenes (unique transcripts matched with known proteins). From all  
190 the 92,343 unigenes, 30,706 were found to have homologs in NR database, 22,261 found to  
191 possess functional domains in Pfam database; 18,944 unigenes showed significant matches to  
192 Swiss-Prot database, 22,361 to KOG, 11,190 to KEGG, 10,876 to COG and 12,410 unigenes  
193 were associated with GO terms (Table 2). Taken together, a total of 33,584 unigenes had at least  
194 one significant matches to these databases (Table 2). The unigenes annotated with NR database  
195 accounted for the largest proportion (91.4%), followed by Pfam and Swiss-Prot (Fig. 2).

196 Distribution of the 12,140 unique proteins in different GO categories is shown Fig. 3. The  
197 transcriptome was enriched in cell component GO categories related to cell part (22.8%) and cell  
198 (22.6%). For biological process, metabolic process (28.1%) was the most abundant GO  
199 categories. Regarding to molecular function, catalytic activity (45.5%) and binding (39.0%) were  
200 the most abundant GO categories. In the correlational study, Du et al. found that membrane-  
201 bounded organelle was the most represented GO term in cell component; the major category in  
202 biological process was the primary metabolic process; and genes involved in hydrolase activity  
203 accounted for major proportion in molecular function. To be noted, due to the samples used in  
204 Du et al. study were collected from different developmental stages and adult tissues (intestines,  
205 respiratory trees and coelomic fluid), there may be some biases.

## 206 **Identification of DEGs**

207 A total of 1,059 DEGs were identified between the papilla and skin. The MA plot showed  
208 significant DGE (blue) against all non-significant DEG (red) (Fig. 4A). Among identified DEGs,  
209 739 were expressed at significantly higher in papilla, while 320 genes were expressed at  
210 significantly higher levels in skin (TableS2). The number of genes with higher expression levels  
211 in papilla was over twice than the number of that in skin. Papilla, as the projections of body wall,  
212 included more unique contents than skin, such as the calcareous ossicles, which are hidden in the

213 dermis of body wall, papillae and tentacles (Steven, Purcell & Chantal, 2012). We also analysed  
214 the expression profiles of 1,059 DEGs in each tissue. Papilla-specific genes represent the DEGs  
215 that there is no expression in the skin, and that goes for skin-specific. A total of 288 papilla-  
216 specific DEGs were expressed only in papilla, while 171 DEGs were found to be only expressed  
217 in skin (skin-specific). A total of 600 DEGs were expressed in both papilla and skin (Fig. 4B).  
218 Apparently, the number of skin-specific (53.44%) genes is higher than papilla-specific genes  
219 (38.97%).

220 Of the 1,059 DEGs, 61 DEGs were annotated to homologous genes in *strongylocentrotus*  
221 *purpuratus*, a model species that is closely related to *A. japonicus*. *Hsp gp96*, *Hsp26*, *ALDOA*  
222 (aldolase class-1 protein) and *tenascin* were annotated with *A. japonicus*. Our results revealed  
223 that *Hsp gp96* and *ALDOA* were 3.93- and 4.45-Fold up-regulated in papillae, respectively. In  
224 contrast, *Hsp26* and *tenascin* were -2.39- and -3.62-Fold down-regulated in skin, respectively.  
225 In addition, 236 differentially expressed genes were not annotated with any database, 160 of  
226 which were apparently higher in papilla. Further analysis revealed that 40 of which were papilla-  
227 specific and two were skin-specific.

228 Putative genes related to development that may be associated with the formation of the  
229 papilla were identified (Table 3). Detailed information of develop-related genes was provided in  
230 Table S3. Our results revealed that *cuticle collagen 2* and *alpha-2 collagen* were highly  
231 expressed in papilla with 5.76 and 2.55, respectively. Several genes that know to be related to the  
232 collagen development (Hinz et al., 2003, 2009; Leask& Abraham, 2004), such as *fibroblast*  
233 *growth factor (FGF)*, *transforming growth factor- $\beta$  (TGF- $\beta$ )* and *integrin- $\alpha$ 2 (ITGA2)* were  
234 found to be significantly expressed. Several *Ras*-related genes such as *Ran*, *Rab1a*, *Arf3*,  
235 *Ran1*, *Ras*, *RhoA*, *Rho Guanine nucleotide exchange factors (RhoGEF)*, Rho GTPase, Rho  
236 GTPase activation protein (RhoGAP) and Ran-binding protein 1 (RanBP1), which play key roles  
237 in the development by regulating growth and morphogenesis, were also identified in our study  
238 (Table S4). All *Ras*-related DEGs were expressed at lower levels in skin except for *RhoGEFs*  
239 that were reported to be associated with cancer, pathogen infection or neural system related

240 diseases and development (Reichman et al., 2015). Understanding of the function of *Ras*-related  
241 genes will facilitate to unravel the mechanisms of some physiological and pathological process  
242 in the skin of *A. japonicus*.

243 To further verify DEGs data, we compared our results with those DEGs identified in the  
244 intestine of *A. japonicus* from a previous study (Sun et al., 2013) (results are shown in Table 4).  
245 7 DEGs showed the same score trend as that of fold change in papilla. The reason for this  
246 observation could be due to the lack of a complete RPKM data (Sun et al., 2013).

#### 247 **qRT-PCR validation**

248 To validate the DEGs results obtained, we randomly selected 16 DEGs for validation using  
249 qRT-PCR. As shown in Fig. 5, the DGEs identified from qRT-PCR analysis were correlated well  
250 with those obtained from qRT-PCR, indicating the reliability and accuracy of the RNA-Seq  
251 method used in the present study.

#### 252 **Enrichment analysis of DEGs**

253 A total of 296 DEGs identified were mapped to 133 pathways. KEGG enrichment pathway  
254 analysis was also carried out to investigate their potential functional roles. The top 10 enrichment  
255 pathways were selected by a hypergeometric test ( $p < 0.05$ ) (Table 5). One of which is the  
256 ribosome pathway, which was related to the protein biogenesis and was observed to be involved  
257 in intestine regeneration (Sun et al., 2013) and aestivation (Chen et al., 2013; Zhao et al., 2014)  
258 in the *A. japonicus*. In addition, tight junction and p53 signaling pathway were also detected in  
259 enrichment pathways analysis (detailed information is provided in Table S5).

#### 260 **DISCUSSION**

261 In this study, we conducted comparative transcriptome analysis between papilla and skin,  
262 two important organs of sea cucumber. A total of 1,059 differentially expressed genes were  
263 identified between the two organs. This result lay the foundation to identify genes that were  
264 potentially involved in the development of the papilla and skin. The generated genomic resources  
265 should be valuable for other genetic and genomic studies in the *A. japonicus*.

266 As previously reported, excessive deposition resulting from abnormal balance of growth

267 factors and cell proliferation can improve local hyperplastic collagen production in skin in  
268 response to injury in mammals (Tuan & Nichte, 1998). Keloids (Seifert & Mrowietz, 2009;  
269 Shih & Bayat, 2010) and hypertrophic scar (HS) (O'Leary, Wood & Guillou, 2002), are  
270 characterized by fibroblastic proliferation and accumulation of extracellular matrix (ECM),  
271 especially excessive deposition of collagen. However, such prominences are regarded as benign  
272 tumors (Diao et al., 2011). It has been suggested that factors such as *FGF*, *ITGA2*, *TGF* and *S-*  
273 *adenosylmethionine (a-SMA)* can cause those lesions (Hinz et al., 2003, 2009; Leask & Abraham,  
274 2004). The FGF activity was first identified from bovine pituitary in 1974 (Gospodarowicz &  
275 Moran, 1974). *FGF* signaling is required for different developmental stages during  
276 embryogenesis (Sun et al. 1999; Naiche et al., 2011; Niwa et al., 2011; Vega-Hernández et al.,  
277 2011). Compared with normal dermal fibroblast, *TGF-β* is believed to induce collagen  
278 production and increase the contractile activity in keloid fibroblasts (Bran et al., 2010;  
279 Sandulache, Parekh & Li-Korotky, 2007). In addition, *TGF-β* associated with *connective tissue*  
280 *growth factor (CCN2)* has been revealed to stimulate *a-SMA*, *collagen* expression (Jiang et al.,  
281 2008). *ITGA2* is the main cell adhesion molecule that takes part in the modulation of collagen  
282 contraction and the activity of myofibroblast in HS (Cooke, Sakai & Mosher, 2000). The  
283 expression levels of *ITGA2* were also found up-regulated in hypertrophic scar fibroblasts,  
284 compared with normal skin tissues in human. In our study, we found that *col-α2* was expressed  
285 at a higher level in the papilla, and we also observed differential expression patterns of genes  
286 involved in collagen synthesis as the major differences between the papilla and skin. The  
287 expression of *FGF*, *TGF-β* and *ITGA2*, associated with collagen development, were all  
288 expressed at higher levels in the papilla. Compare to previous studies of local hyperplastic  
289 collagen in mammals, we speculate that these collagen-related genes may play critical roles in  
290 stimulating the production of collagen in papilla and might be involved in the morphological  
291 differentiation between the two organs.

292 Besides the development-related genes as discussed above, some immune-related genes are

293 also identified to be differentially expressed between papilla and skin in this study such as  
294 *Hspgp96*, *Hsp26*, *ALDOA* and *tenascin*. Many lines of evidences support that Hsps act as natural  
295 immunoregulatory agents, increasing the awareness of innate immune cells to pathogens  
296 (Ciancio&Chang, 2008; Prohaszka&Fust, 2004; Zugel& Kaufmann, 1999). *ALDOA* plays a role  
297 in glycolysis pathway (Oparina et al., 2013). Further investigation is required to explore the  
298 pathological researches for papilla and skin. Through analysis of the DEGs against intestine  
299 transcriptome data from a previous study (Sun et al., 2013). *Fibrinogen-like protein A (fglA)*, a  
300 member of the fibrinogen-related protein superfamily, plays crucial roles including innate  
301 immune response, regeneration and blood clotting (Yamamoto et al., 1993). Previous studies  
302 have demonstrated that *fglA* is widely distributed in *A. japonicus* body wall, intestines,  
303 longitudinal muscles and respiratory tree of *A. japonicus* (Wu et al., 2014). Our results also show  
304 that *fglA* was 3.02 fold change and 4.96 score up-regulated in papilla, respectively. The role of  
305 *fglA* in the development of papilla remains unclear and further investigation is required to  
306 understand its functional roles.

307 Enrichment KEGG analysis revealed that tight junction and p53 signaling pathway were  
308 highlighted in enrichment pathways. In human, the content of G2-M arrested cells in keloid skin  
309 was higher than normal skin (Shohreh et al., 2011). Keloid fibroblasts showed a higher rate of  
310 senescence and lower proliferative capacity in comparison to normal fibroblasts (Shohreh et al.,  
311 2011). In our study, a set of genes, including growth arrest and DNA-damage-inducible protein  
312 (*gadd45*), cyclin dependent kinase 1 (*cdk*), cyclin-B (*cyc-B*), cyclin-A (*cyc-A*) and cytochrome C  
313 (*cyt-C*), were all expressed at higher levels in the papilla (Table 1). These genes are involved in  
314 the p53 signaling pathway. Once p53 signaling pathway is activated, it can induce either cell  
315 cycle arrest or apoptosis in the damaged cell. In humans, *cyc-B* and *cdk2* kinase influence a cell's  
316 progress through the cell cycle, which is especially important in several skin cancers (Ely et al.,  
317 2005; Casimiro et al., 2014). *Cyc-B* forms the regulatory subunits and *cdk2* form the catalytic  
318 subunits of an activated heterodimer. The *cyc-B* has no catalytic activity, and *cdk2* is inactive in  
319 the absence of a partner *cyc-B*. Once activated the *cdk2/cyc-B* complex control cell cycle (Abreu,

320 Velez & Howard, 2015). Gadd45 is a ubiquitously expressed 21 protein with a key role in  
321 response to genotoxic agents, and it is involved in many biological processes related to  
322 maintenance of genomic stability and apoptosis. It has been shown that gadd45's inhibits cdk2  
323 kinase activity through alteration of cyc-B subcellular localization, inducing the arrest of the cell  
324 cycle in G2-M state (Jin et al., 2000; Smith et al., 1994). These results indicated that the level of  
325 cell cycle arrest at the G2-M in the papilla might be higher than in the skin. It's speculated that  
326 papilla fibroblasts commit to a higher rate of senescence, which may cause fibroblast-related  
327 genes eventually stop expressing and maintain external morphology of the papilla.

328 Genes involved in tight junction were enriched in papilla. Tight junctions are essential for  
329 epithelial morphology, which can form seals between epithelial cells and create a selectively  
330 permeable barrier to intercellular diffusion (Zheng et al., 2011). Besides, we also found that the  
331 expression of Serine/threonine-protein phosphatase (PP2A) in papilla is higher than that in the  
332 skin. Many reports showed that PP2A regulates *saxia telangiectasia mutated (ATM)*, *ataxia*  
333 *telangiectasia Rad3 related (ATR)*, *check point kinase-1 (CHK1)*, and *checkpoint kinase-2*  
334 *(CHK2)* after DNA damage, and activate the checkpoint of G2-M associated with the p53  
335 signaling pathway. The process activated by PP2A may also regulate the external morphological  
336 of papilla and skin of *A. japonicus*.

### 337 CONCLUSION

338 In this study, we performed comparative transcriptome analysis of the skin and papilla *A.*  
339 *japonicus* by using RNA-Seq. In total, 156,501 transcripts and 92,343 unigenes were assembled.  
340 A total of 1,059 differentially expressed genes were identified between the two important  
341 organs of *A. japonicus*. We identified 236 novel genes (not annotated with any database), 160 of  
342 which were expressed at higher levels in papilla. Further tissue-expression analysis identified  
343 288 papilla-specific genes and 171 skin-specific genes. Gene pathway enrichment analysis  
344 revealed several gene pathways that were involved in development. In addition, many DEGs  
345 involved in the process of p53 signaling pathway and tight junction were also identified, which  
346 were reported to be relative to keloid skin in human. This result provided insights into genes and

347 pathways that may be associated with the formation of the papilla and skin in sea cucumber,  
348 laying foundation for further investigation to understand the development of the papilla in *A.*  
349 *japonicus*. Moreover, the generation of larger-scale transcriptomic data presented in this work  
350 enriched genetic resources of echinodermata species, which should be valuable to comparative  
351 and evolutionary studies in echinoderms.

352

### 353 ACKNOWLEDGEMENTS

354 We thank Dr. Daniel Garcia de la serrana (Fish Muscle Research Group, Scottish Oceans  
355 Institute, University of St Andrews, UK) for revising and polishing the manuscript. We would  
356 like to acknowledge Prof. Tzi Bun Ng and two anonymous reviewers for helpful comments on  
357 the manuscript.

### 358 REFERENCES

- 359 **Abreu, Velez AM, Howard MS. 2015.** Tumor-suppressor Genes, Cell Cycle Regulatory  
360 Checkpoints, and the Skin. *N Am J Med Sci* 7:176–188 DOI: 10.4103/1947-2714.157476.
- 361 **Adibzadeh N, Aminzadeh S, Jamili S, Karkhane AA, Farrokhi N. 2014.** Purification and  
362 characterization of pepsin-solubilized collagen from skin of sea cucumber *Holothuria parva*.  
363 *Appl Biochem Biotechnol* 173:143-54 DOI: 10.1007/s12010-014-0823-4.
- 364 **Anisimov SV. 2008.** Serial Analysis of Gene Expression (SAGE): 13 years of application in  
365 research. *Curr Pharm Biotechnol* 9:338–50 DOI: 10.2174/138920108785915148.
- 366 **Bran GM, Sommer UJ, Goessler UR, Hörmann K, Riedel F, Sadick H. 2010.** TGF- $\beta$ 1  
367 antisense impacts the SMAD signalling system in fibroblasts from keloid scars. *Anticancer*  
368 *Res* 30:3459–3463.
- 369 **Casimiro MC, Velasco-Velázquez M, Aguirre-Alvarado C, Pestell RG. 2014.** Overview of  
370 cyclins D1 function in cancer and the CDK inhibitor landscape: Past and present. *Expert*  
371 *Opin Investig Drugs* 23:295-304 DOI: 10.1517/13543784.2014.867017.
- 372 **Chang Y, Ding J, Song J, Yang W. 2004.** *Biology and Aquaculture of Sea Cucumbers and Sea*  
373 *Urchins*. Ocean Press, Beijing, China. 35-38. (in Chinese)

- 374 **Chang YQ, Zhu F, Yu J, Ding J. 2009.** Genetic variability analysis in five populations of the  
375 sea cucumber *Stichopus (Apostichopus japonicus)* from China, Russia, South Korea and  
376 Japan as revealed by microsatellite markers. *Marine Ecology* **30**:455–461 DOI:  
377 10.1111/j.1439-0485.2009.00292.x.
- 378 **Chang YQ, Shi SB, Zhao C, Han ZH. 2011.** Characteristics of papillae in wild, cultivated and  
379 hybrid sea cucumbers (*Apostichopus japonicus*). *African Journal of Biotechnology*  
380 **10**:13780–13788.
- 381 **Ciancio MJ, Chang EB. 2008.** Do heat shock proteins play any role in gut inflammation?  
382 *Inflamm Bowel Dis* **14**:S102e3 DOI: 10.1002/ibd.20697.
- 383 **Cooke ME, Sakai T, Mosher DF. 2000.** Contraction of collagen matrices mediated by  $\alpha 2$   
384 beta1A and  $\alpha$  (v) beta3 Ins. *J Cell Sci* **113**:375–83
- 385 **Cui J, Liu S, Zhang B, Wang H, Sun H, Song S, Qiu X, Liu Y, Wang X, Jiang Z, Liu Z.**  
386 **2014.** Transcriptome Analysis of the Gill and Swimbladder of *Takifugurubripes* by RNA-  
387 Seq. *PLoS ONE* **9**, e85505 DOI: 10.1371/journal.pone.0085505.
- 388 **Cui J, Xu J, Zhang S, Wang K, Jiang Y, Mahboob S, Al-Ghanim KA, Xu P. 2015.**  
389 Transcriptional Profiling Reveals Differential Gene Expression of Amur Ide (*Leuciscus*  
390 *waleckii*) during Spawning Migration. *Int J Mol Sci* **16**:13959-13972 DOI:  
391 10.3390/ijms160613959.
- 392 **Diao JS, Xia WS, Yi CG, Wang YM, Li B, Xia, W Liu, B, Guo SZ, Sun XD. 2011.**  
393 Trichostatin A inhibits collagen synthesis and induces apoptosis in keloid fibroblasts. *Arch*  
394 *Dermatol Res* **303**:573–580 DOI: 10.1007/s00403-011-1140-1.
- 395 **Du H, Bao Z, Hou R, Wang S, Su H, Yan J, Tian M, Li M, Wei W, Lu W, Hu X, Wang S,**  
396 **Hu J. 2012.** Transcriptome Sequencing and Characterization for the Sea Cucumber  
397 *Apostichopus japonicus* (Selenka, 1867). *PLoS ONE* **7**:e33311 DOI:  
398 10.1371/journal.pone.0033311.
- 399 **Ely S, Di Liberto M, Niesvizky R, Baughn LB, Cho HJ, Hatada EN, Knowles DM, Lane J,**  
400 **Chen-Kiang S. 2005.** Mutually exclusive cyclin-dependent kinase 4/cyclin D1 and cyclin-

- 401 dependent kinase 6/cyclin D2 pairing inactivates retinoblastoma protein and promotes cell  
402 cycle dysregulation in multiple myeloma. *Cancer Res* **65**:11345-53 DOI: 10.1158/0008-  
403 5472.CAN-05-2159.
- 404 **Fuess LE, Eisenlord ME, Closek CJ, Tracy AM, Mauntz R, Gignoux-Wolfsohn S, Moritsch**  
405 **MM, Yoshioka R, Burge CA, Harvell CD, Friedman CS, Hewson I, Hershberger PK,**  
406 **Roberts SB. 2015.** Up in Arms: Immune and Nervous System Response to Sea Star  
407 Wasting Disease. *PLoS One* **10**:e0133053 DOI: 10.1371/journal.pone.0133053.
- 408 **Gao Q, Liao M, Wang Y, Li B, Zhang Z, Rong X, Chen G, Wang L. 2015.** Transcriptome  
409 Analysis and Discovery of Genes Involved in Immune Pathways from Coelomocytes of Sea  
410 Cucumber (*Apostichopus japonicus*) after *Vibrio splendidus* Challenge. *Int J Mol Sci*  
411 **16**:16347-77 DOI: 10.3390/ijms160716347.
- 412 **Gospodarowicz D, Moran J. 1974.** Effect of a fibroblast growth factor, insulin, dexamethasone,  
413 and serum on the morphology of BALB/c 3T3 cells. *Proc Natl Acad Sci* **71**:4648-52
- 414 **Grabherr MG, Haas BJ, Yassour M, Levin JZ, Thompson DA, Amit I, Adiconis X, Lin**  
415 **Raktima Raychowdhury, Zeng Q, Chen Z, Mauceli E, Hacohen N, Gnirke A, Rhind N,**  
416 **Pama F, Birren BW, Nusbaum C, Lindblad-Toh L, Friedman N & Regev A. 2011.**  
417 Full-length transcriptome assembly from RNA-Seq data without a reference genome.  
418 *Nature Biotechnology* **29**:644–652 DOI:10.1038/nbt.1883.
- 419 **Hinz B. 2009.** Tissue stiffness, latent TGF- $\beta$ 1 activation, and mechanical signal transduction:  
420 implications for the pathogenesis and treatment of fibrosis. *Curr Rheumatol Rep* **11**:120–6  
421 DOI: 10.1007/s11926-009-0017-1
- 422 **Hinz B, Dugina V, Ballestrem C, Wehrle-Haller B, Chaponnier C. 2003.** Alpha-smooth  
423 muscle actin is crucial for focal adhesion maturation in myofibroblasts. *Mol Biol Cell*  
424 **14**:2508–19 DOI: 10.1091/mbc.E02-11-0729
- 425 **Hyman LH. 1955.** *The Invertebrates, Vol 4 Echinodermata*. New York: McGraw-Hill, 763.
- 426 **Jiang D, Jiang Z, Han F, Zhang Y, Li Z. 2008.** HGF suppresses the production of collagen  
427 type III and alpha-SMA induced by TGF-beta1 in healing fibroblasts. *Eur J Appl Physiol*

- 428       **103**:489-93 DOI: 10.1007/s00421-008-0733-7.
- 429 **Jin S, Antinore MJ, Lung FD, Dong X, Zhao H, Fan F, Colchagie AB, Blanck P, Roller PP,**  
430 **Fornace Jr, Zhan Qimin. 2000.** The GADD45 inhibition of Cdc2 kinase correlates with  
431 GADD45-mediated growth suppression. *J Biol Chem* **275**:16602-16608 DOI:  
432 10.1074/jbc.M000284200.
- 433 **Leask A, Abraham DJ. 2004.** TGF- $\beta$  signaling and the fibrotic response. *FASEB J* **18**, 816–27  
434 DOI:10.1096/fj.03-1273rev.
- 435 **Li C, Feng W, Qiu L, Xia C, Su X, Jin C, Zhou T, Li T. 2012.** Characterization of skin  
436 ulceration syndrome associated microRNAs in sea cucumber *Apostichopus japonicus* by  
437 deep sequencing. *Fish Shellfish Immunol* **33**:436-41 DOI: 10.1016/j.fsi.2012.04.013.
- 438 **Liu H, Zheng F, Sun X, Hong X, Dong S, Wang B, Tang X, Wang Y. 2010.** Identification of  
439 the pathogens associated with skin ulceration and peristome tumescence in cultured sea  
440 cucumbers *Apostichopus japonicus* (Selenka). *Journal of Invertebrate Pathology* **105**:236–  
441 242 DOI: 10.1016/j.jip.2010.05.016.
- 442 **Livak KJ, Schmittgen TD. 2001.** Analysis of Relative Gene Expression Data Using Real-Time  
443 Quantitative PCR and the  $2^{-\Delta\Delta Ct}$ . *Method Methods* **25**:402–408  
444 DOI:10.1006/meth.2001.1262.
- 445 **Lowdon RF, Zhang B, Bilenky M, Mauro T, Li D, Gascard P, Sigaroudinia M, Farnham**  
446 **PJ, Bastian BC, Tlsty TD, Marra MA, Hirst M, Costello JF, Wang T, Cheng JB. 2014.**  
447 Regulatory network decoded from epigenomes of surface ectoderm-derived cell types. *Nat*  
448 *Commun* **25**:5442 DOI: 10.1038/ncomms6442.
- 449 **Luke A, Hoekstra Leonid L, Moroz, Heyland A. 2012.** Novel Insights into the Echinoderm  
450 Nervous System from Histaminergic and FMRFaminergic-Like Cells in the Sea Cucumber  
451 *Leptosynapta clarki*. *PLoS One* **7**:e44220 DOI: 10.1371/journal.pone.0044220.
- 452 **Chen M, Zhang X, Liu J, Storey KB. 2013.** High-throughput sequencing reveals differential  
453 expression of miRNAs in intestine from sea cucumber during aestivation. *PLoS One*.  
454 **15**;8(10):e76120 DOI: 10.1371/journal.pone.0076120.

- 455 **Naiche LA, Holder N, Lewandoski M. 2011.** FGF4 and FGF8 comprise the wavefront activity  
456 that controls somitogenesis. *ProcNatlAcad Sci* **108**:4018–4023 DOI:  
457 10.1073/pnas.1007417108.
- 458 **Niwa Y, Shimojo H, Isomura A, González A, Miyachi H, Kageyama R. 2011.** Different types  
459 of oscillations in Notch and Fgf signaling regulate the spatiotemporal periodicity of  
460 somitogenesis. *Genes* **25**:1115–1120 DOI: 10.1101/gad.2035311.
- 461 **Oparina NY, Snezhkina AV, Sadritdinova AF, Veselovskii VA, Dmitriev AA, Senchenko**  
462 **VN, Mel'nikova NV, Speranskaya AS, Darii MV, Stepanov OA, Barkhatov IM,**  
463 **Kudryavtseva AV. 2013.** Differential expression of genes that encode glycolysis enzymes  
464 in kidney and lung cancer in humans. *Genetika* **49**:814-23.
- 465 **O'Leary R, Wood EJ, Guillou PJ. 2002.** Pathological scarring: strategic interventions. *Eur J*  
466 *Surg* **168**:523–34 DOI: 10.1002/ejs.6161681002.
- 467 **Prohaszka Z, Fust G. 2004.** Immunological aspects of heat-shock proteins-the optimum stress of  
468 life. *Mol Immunol* **41**:29e44 DOI:10.1016/J.MOLIMM.2004.02.00.
- 469 **Reichman M, Schabdach A, Kumar M, Zielinski T, Donover PS, Laury-Kleintop LD,**  
470 **Lowery RGA. 2015.** High-Throughput Assay for Rho Guanine Nucleotide Exchange  
471 Factors Based on the Transcreeper GDP Assay. *J Biomol Screen* DOI:  
472 101177/1087057115596326.
- 473 **Runcie DE, Garfield DA, Babbitt CC, Wygoda JA, Mukherjee S, Wray GA. 2012.** Genetics  
474 of gene expression responses to temperature stress in a sea urchin gene network *Mol Ecol*  
475 **21**:4547-62 DOI: 10.1111/j.1365-294X.2012.05717.x.
- 476 **Sandulache VC, Parekh A, Li-Korotky H. 2007.** Prostaglandin E2 inhibition of keloid  
477 fibroblast migration, contraction, and transforming growth factor (TGF)-beta1-induced  
478 collagen synthesis. *Wound Repair Regen* **15**:122–133 DOI: 10.1111/j.1524-  
479 475X.2006.00193.x.
- 480 **Seifert O, Mrowietz U. 2009.** Keloid scarring: bench and bedside. *Arch Dermatol Res*  
481 **301**:259–272 DOI: 10.1007/s00403-009-0952-8.

- 482 **Shih B, Bayat A. 2010.** Genetics of keloid scarring. *Arch Dermatol Res* **302**:319–339 DOI:  
483 10.1007/s00403-009-1014-y.
- 484 **Sloan NA. 1984.** B F Keegan, B D S O'Connor, Eds. *Echinoderm fisheries of the world: a*  
485 *review In Echinodermata: Proceedings of the 5th International Echinoderm Conference,*  
486 Balkema, Rotterdam, The Netherlands, 109–124.
- 487 **Smith ML, Chen IT, Zhan Q, Bae I, Chen CY, Gilmer TM, Kastan MB, O'Connor PM,**  
488 **Fornace AJ. 1994.** Interaction of the p53-regulated protein Gadd45 with proliferating cell  
489 nuclear antigen. *Science* **266**:1376-1380 DOI:10.1126/science.7973727.
- 490 **Steven W, Purcell Yves S, Chantal C. 2012.** *Commercially Important Sea Cucumber of The*  
491 *World.* FAO Species Catalogue for Fishery Purposes: Rome, pp2, 3, 4, 6, 11, 86.
- 492 **Sun L, Chen M, Yang H, Wang T, Liu B, Shu C, Gardiner DM. 2011.** Large scale gene  
493 expression profiling during intestine and body wall regeneration in the sea cucumber  
494 *Apostichopus japonicas*. *Comp BiochemPhysiol Part D Genomics Proteomics* **6**:195-205  
495 DOI: 10.1016/j.cbd.2011.03.002.
- 496 **Sun L, Yang H, Chen M, Ma D, Lin C. 2013.** RNA-Seq Reveals Dynamic Changes of Gene  
497 Expression in Key Stages of Intestine Regeneration in the Sea Cucumber *Apostichopus*  
498 *japonicas*. *PLoS ONE* **8**:e69441 DOI: 10.1371/journal.pone.0069441.
- 499 **Sun X, Meyers EN, Lewandoski M, Martin GR. 1999.** Targeted disruption of Fgf8 causes  
500 failure of cell migration in the gastrulating mouse embryo. *Genes* **13**:1834–1846 DOI:  
501 10.1101/gad.13.14.1834.
- 502 **Tu Q, Cameron RA, Worley KC, Gibbs RA, Davidson EH. 2012.** Gene structure in the sea  
503 urchin *Strongylocentrotus purpuratus* based on transcriptome analysis. *Genome Res*  
504 **22**:2079-87 DOI: 10.1101/gr.139170.112.
- 505 **Tuan TL, Nichter LS. 1998.** The molecular basis of keloid and hypertrophic scar formation.  
506 *Mol Med Today* **4**:19–24 DOI: 10.1016/S1357-4310(97)80541-2. DOI: 10.1016/S1357-  
507 4310(97)80541-2.
- 508 **Vanden-Spiegel D, Flammang P, Fourmeau D, Jangoux M. 1995.** Fine structure of the dorsal

- 509 papillae in the holothurioid *Holothuriaforskali* (Echinodermata). *Tissue Cell* **27**, 7-465  
510 DOI:10.1016/S0040-8166(95)80066-2.
- 511 **Varmeh S, Egia A, McGrouther D, Tahan SR, Bayat A, Pandolfi PP. 2011.** Cellular  
512 Senescence as a Possible Mechanism for Halting Progression of Keloid Lesions. *Genes*  
513 *Cancer* **2**:1061–1066 DOI: 10.1177/1947601912440877.
- 514 **Vega-Hernández M, Kovacs A, De Langhe S, Ornitz DM. 2011.** FGF10/FGFR2b signaling is  
515 essential for cardiac fibroblast development and growth of the myocardium *Development*  
516 **138**:3331–3340 DOI: 10.1242/dev.064410.
- 517 **Wang Z, Gerstein M, Snyder M. 2009.** RNA-Seq: a revolutionary tool for transcriptomics. *Nat*  
518 *Rev Genet* **10**:57–63 DOI: 10.1038/nrg2484.
- 519 **Wang H, Zhang W Li, C Lv Z, Jin C. 2015.** Identification and characterization of a novel Foxo  
520 transcription factors in *Apostichopus japonicas*. *Fish Shellfish Immunol* **44**: 164-71 DOI:  
521 10.1016/j.fsi.2015.02.006.
- 522 **Wu Y, Yao F, Mei Y, Chu B, Cheng C, Liu Y, Li X, Zou X, Hou L. 2014.** Cloning and  
523 expression analysis of the gene encoding fibrinogen-like protein A, a novel regeneration-  
524 related protein from *Apostichopus japonicas*. *Mol Biol Rep* **41**:2617-27. DOI:  
525 10.1007/s11033-014-3120-y.
- 526 **Yamamoto T, Gotoh M, Sasaki H, Terada M, Kitajima M, Hirohashi S. 1993.** Molecular  
527 cloning and initial characterization of a novel fibrinogen-related gene, HFREP-1. *Biochem*  
528 *Biophys ResCommun* **193**:681–687 DOI:10.1006/bbrc.1993.1678.
- 529 **Yang L, Li C, Chang Y, Gao Y, Wang Y, Wei J, Song J, Sun P. 2015.** Identification and  
530 characterization a novel transcription factor activator protein-1 in the sea cucumber  
531 *Apostichopus japonicas*. *Fish Shellfish Immunol* **45**:927-32 DOI: 10.1016/j.fsi.2015.06.015.
- 532 **Zhang P, Li C, Zhu L, Su X, Li Y, Jin C, Li T. 2013.** De Novo Assembly of the Sea Cucumber  
533 *Apostichopus japonicas* Hemocytes Transcriptome to Identify miRNA Targets Associated  
534 with Skin Ulceration Syndrome. *PLoS ONE* **8**:e73506 DOI: 10.1371/journal.pone.0073506.
- 535 **Zhao Y, Yang H, Storey KB, Chen M. 2014.** RNA-seq dependent transcriptional analysis

- 536 unveils gene expression profile in the intestine of sea cucumber *Apostichopus japonicas*.  
537 *Comparative Biochemistry and Physiology, Part D* **10**:30-43 DOI:  
538 10.1016/j.cbd.2014.02.002.
- 539 **Zhao Y, Yang H, Storey KB, Chen M. 2014.** Differential gene expression in the respiratory  
540 tree of the sea cucumber *Apostichopus japonicas* during aestivation. *Marine Genomics*  
541 **18**:173-183 DOI: 10.1016/j.margen.2014.07.001.
- 542 **Zheng W, Wang Z, Collins JE, Andrews RM, Stemple D, Gong Z. 2011.** Comparative  
543 transcriptome analyses indicate molecular homology of zebrafish swimbladder and  
544 mammalian lung. *PLoS One* **6**:e24019 DOI: 10.1371/journal.pone.0024019.
- 545 **Zhou ZC, Dong Y, Sun HJ, Yang AF, Chen Z, Gao S, Jiang JW, Guan XY, Jiang B, Wang**  
546 **B. 2014.** Transcriptome sequencing of sea cucumber (*Apostichopus japonicus*) and the  
547 identification of gene-associated markers. *Molecular Ecology Resources* **14**:127–138 DOI:  
548 10.1111/1755-0998.12147.
- 549 **Zugel U, Kaufmann SH. 1999.** Role of heat shock proteins in protection from and pathogenesis  
550 of infectious diseases. *Clin Microbiol Rev* **12**:19e39 DOI: 10.1088/0965-0393/10/4/303.  
551  
552

**Table 1** (on next page)

Summary of the RNA-Seq data.

1

**Table 1. Summary of the RNA-Seq data.**

	<b>Number of reads</b>	<b>Number of reads after trimming</b>	<b>Number of nucleotides after trimming (bp)</b>
<b>Papilla</b>	33,504,127	30,657,027	7,723,425,469
<b>Skin</b>	37,384,685	36,444,908	9,182,161,309
<b>Total</b>	70,888,812	67,101,935	16,905,586,778

2

**Table 2** (on next page)

Statistics of transcriptome reference assembly and annotation.

1

**Table 2. Statistics of transcriptome reference assembly and annotation.**

	Number of transcripts	156,501
	Maximum transcript length	18,781 bp
	Minimum transcript length	201 bp
<b>Assembly</b>	Average transcript length	910.77bp
	N50 length	1,694bp
	Number of mapped reads from the papilla	25,946,333 (84.6%)
	Number of mapped reads from the skin	30,913,283 (84.8%)
	Unigenes with blast hits to NR	30,706
	Unigenes with blast hits to Pfam	22,261
	Unigeneswith blast hits to Swiss-Prot	18,944
<b>Annotation</b>	Unigeneswith blast hits to KOG	22,361
	Unigeneswith blast hits to COG	10,876
	Unigeneswith KEGG terms	11,190
	Unigeneswith GO terms	12,140
	Total	33,584

2

**Table 3** (on next page)

Differentially expressed genes between the papilla and skin that are involved in development.

1 **Table 3. Differentially expressed genes between the papilla and skin that are involved in**  
 2 **development.**

Unigene ID	Gene symbol	Foldchange
c14695.graph_c0	<i>cdk</i>	4.96
c40875.graph_c0	<i>cyc-B</i>	6.26
c75877.graph_c0	<i>cyc-A</i>	6.346
c76406.graph_c0	<i>cytC</i>	2.76
c76859.graph_c0	<i>gadd45a</i>	4.82
c12901.graph_c0	<i>ck2bl</i>	4.40
c14611.graph_c0	<i>MAGUKs</i>	4.34
c18023.graph_c0	<i>PP2A</i>	4.54
c19039.graph_c0	<i>claudin</i>	6.31
c37832.graph_c0	<i>actin</i>	6.05
c16255.graph_c0	<i>FGF</i>	5.26
c58770.graph_c0	<i>ITGA2</i>	2.12
c15897.graph_c0	<i>TGF-<math>\beta</math></i>	6.21
c54738.graph_c0	<i>col-<math>\alpha</math>2</i>	2.55
c54237.graph_c0	<i>tub-<math>\alpha</math></i>	-4.53
c77661.graph_c0	<i>emmhc</i>	4.49
c54933.graph_c0	<i>eef2</i>	-5.43
c42633.graph_c0	<i>gtf 8</i>	4.96
c57892.graph_c0	<i>ubeE2</i>	-4.18
c76626.graph_c0	<i>ctATPase</i>	4.62
c38162.graph_c0	<i>cul-<math>\alpha</math>2</i>	5.76

3

**Table 4**(on next page)

The result of DEGs with significantly different expression by comparison with the intestine.

1 **Table 4. The result of DEGs with significantly different expression by comparison with the**  
 2 **intestine.**

Unigene ID	Isotig ID	Annotate	Foldchang	Score
c45050.graph_c0	isotig25664	Cell death abnormality protein 1	8.62	14.40
c64723.graph_c0	isotig15743	Sushi domain (SCR repeat)	7.15	4.09
c67657.graph_c0	isotig19241	Fibrinogen-like protein A	3.02	4.96
c66534.graph_c0	isotig15670	hypothetical protein CAPTEDRAFT_211426	2.84	11.35
c73725.graph_c2	isotig27287	Sulfotransferase family	2.56	12.76
c60095.graph_c0	isotig09563	hypothetical protein BRAFLDRAFT_231341	2.54	4.31
c60588.graph_c0	isotig18328	Histone-lysine N-methyltransferase	2.16	13.36

3 The “Isotig ID” column indicates the gene ID from the data of Sun et al. (Sun et al., 2013).  
 4

**Table 5** (on next page)

Enrichment analysis of genes with significantly differential expression between the papilla and skin.

1 **Table 5. Enrichment analysis of genes with significantly differential expression between the**  
 2 **papilla and skin.**

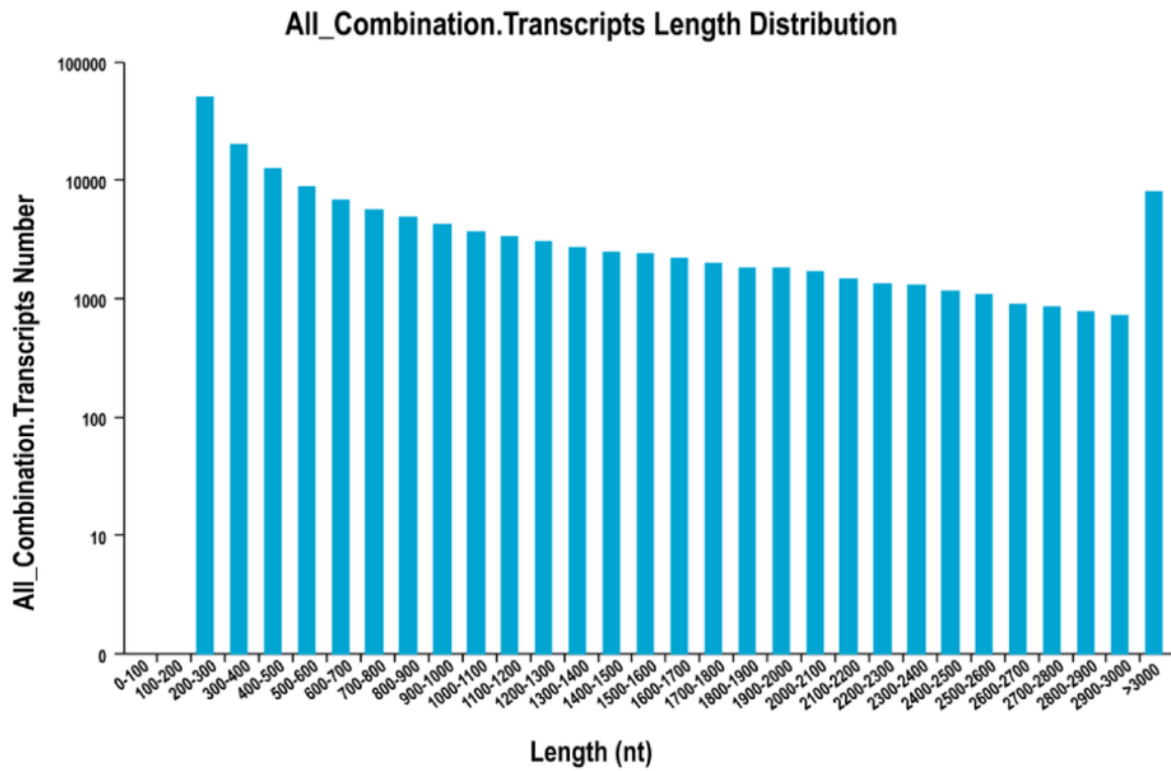
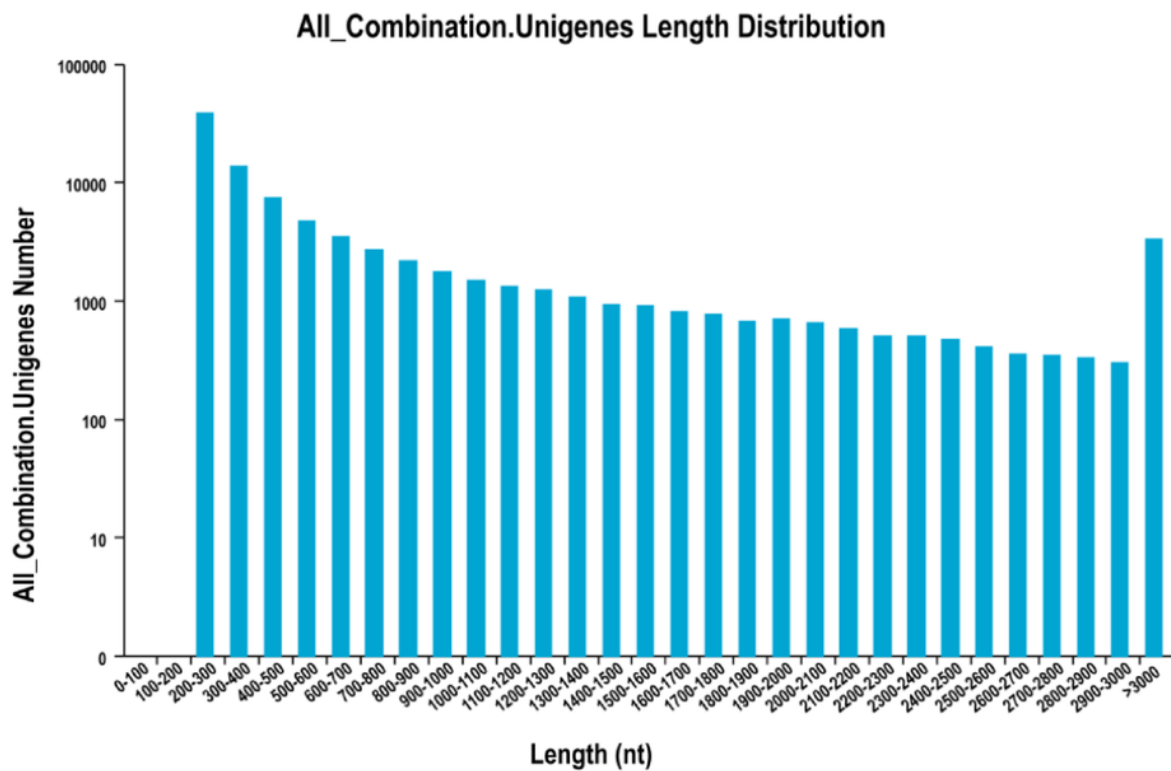
<b>Pathway</b>	<b>KO</b>	<b>Enrichment factor</b>	<b>p-value</b>
Ribosome	ko03010	0.39	1.47E-13
Oocyte meiosis	ko04114	0.27	2.07E-06
Cell cycle	ko04110	0.40	0.000557178
Glycolysis / Gluconeogenesis	ko00010	0.43	0.000610528
p53 signaling pathway	ko04115	0.28	0.003222732
Tight junction	ko04530	0.38	0.004679565
NOD-like receptor signaling pathway	ko04621	0.27	0.010624351
Regulation of actin cytoskeleton	ko04810	0.44	0.017102208
RNA transport	ko03013	0.68	0.029611824
Progesterone-mediated oocyte maturation	ko04914	0.52	0.033017313

3

# 1

The distribution of the size of transcripts and unigenes.

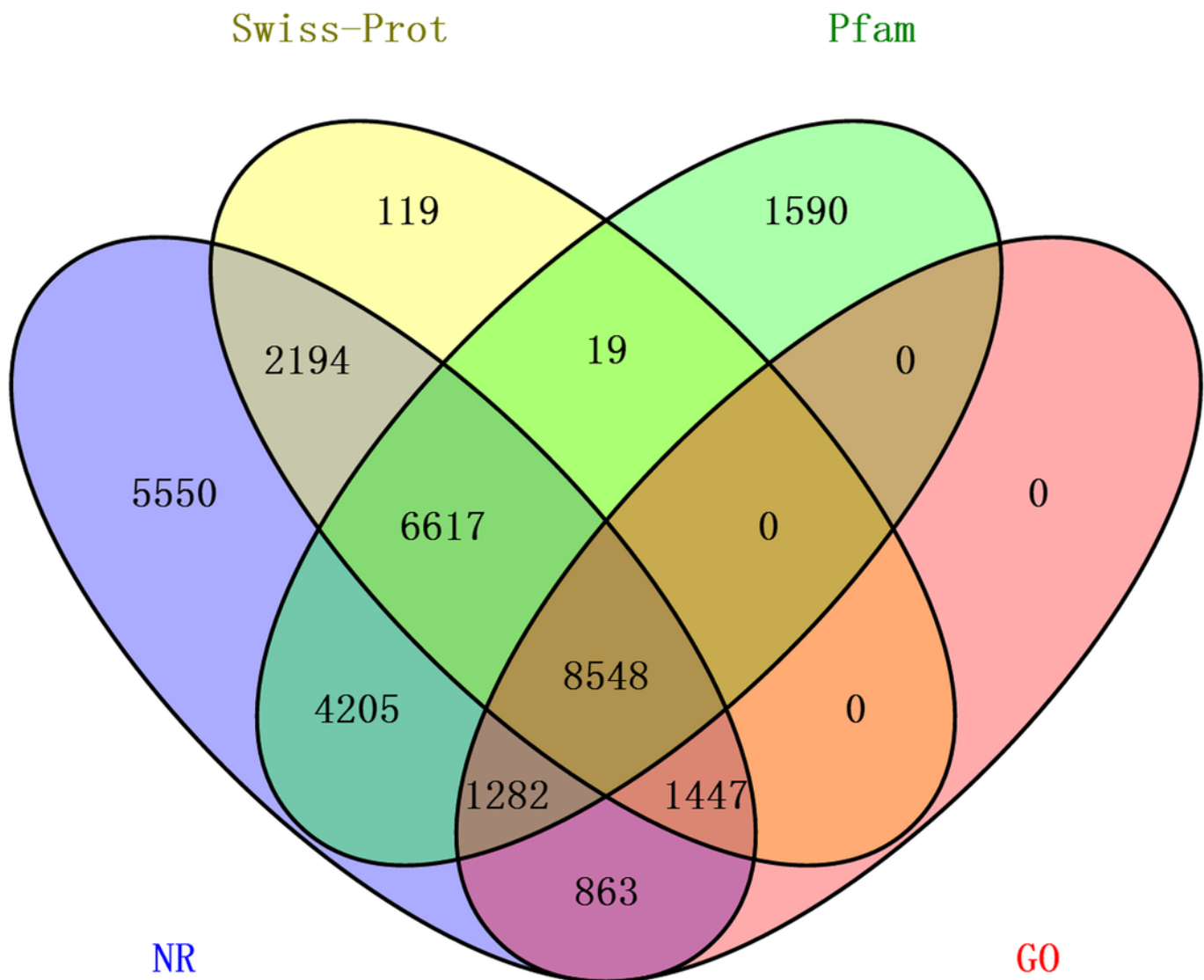
Length distribution of assembled transcripts (A) and unigenes (B) of sea cucumber (*Apostichopus japonicus*).

**A****B**

## 2

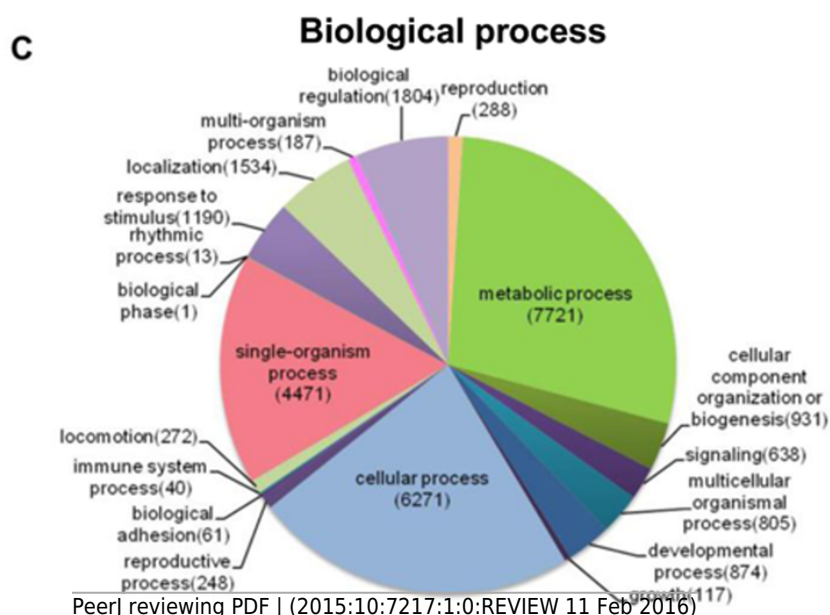
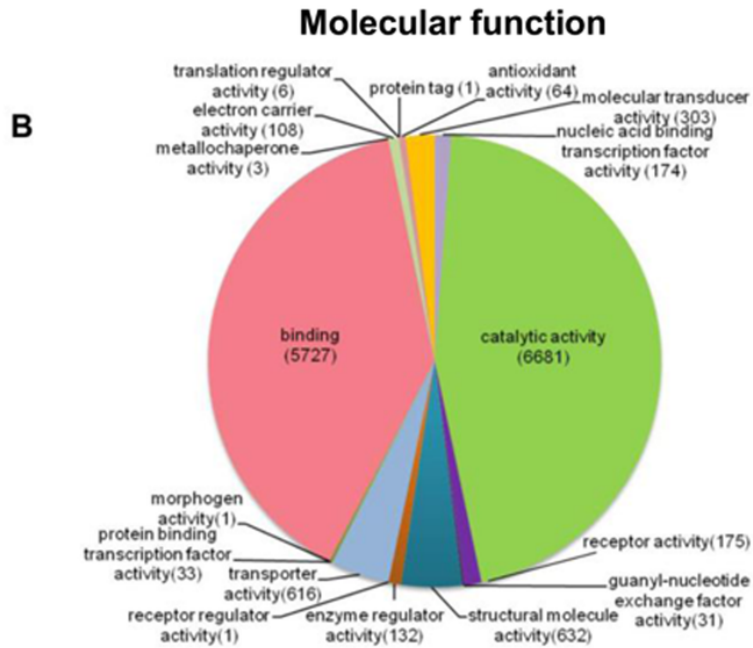
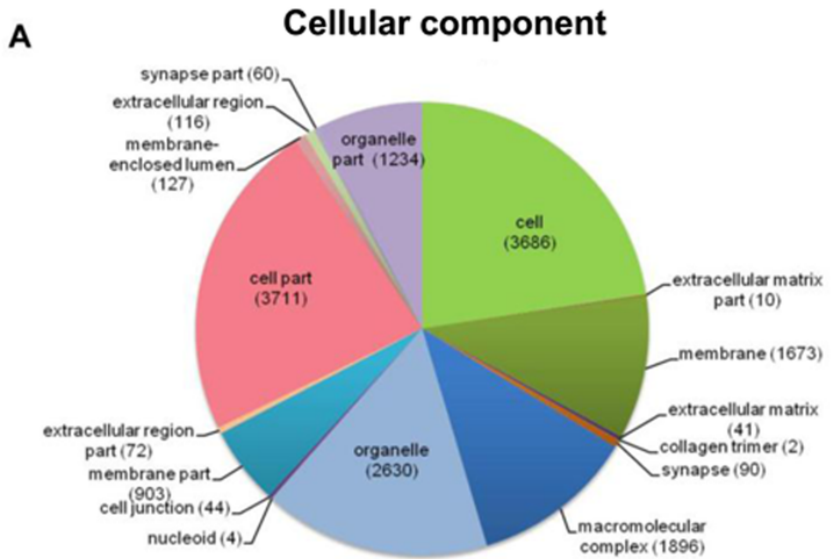
The distribution of annotated unigenes across database.

Venn diagram display of the proportion of annotated unigenes in NR, Pfam, Swiss-Prot and GO.



# 3

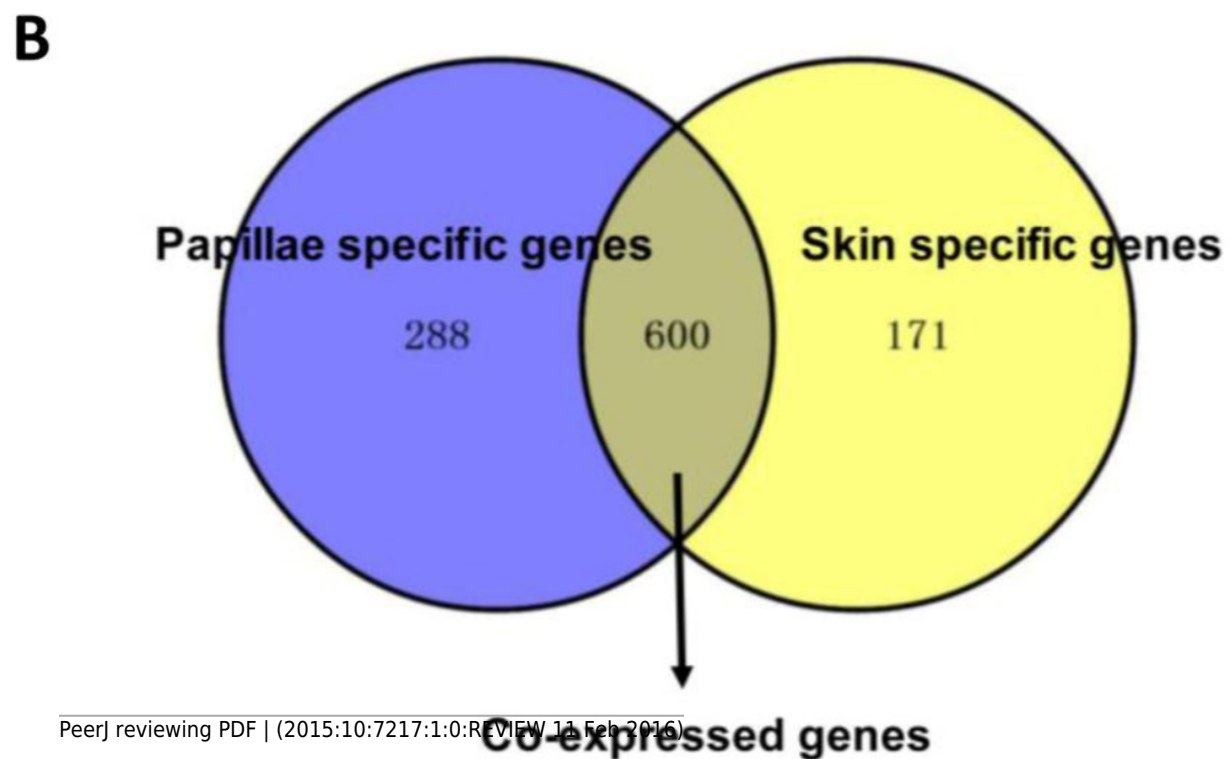
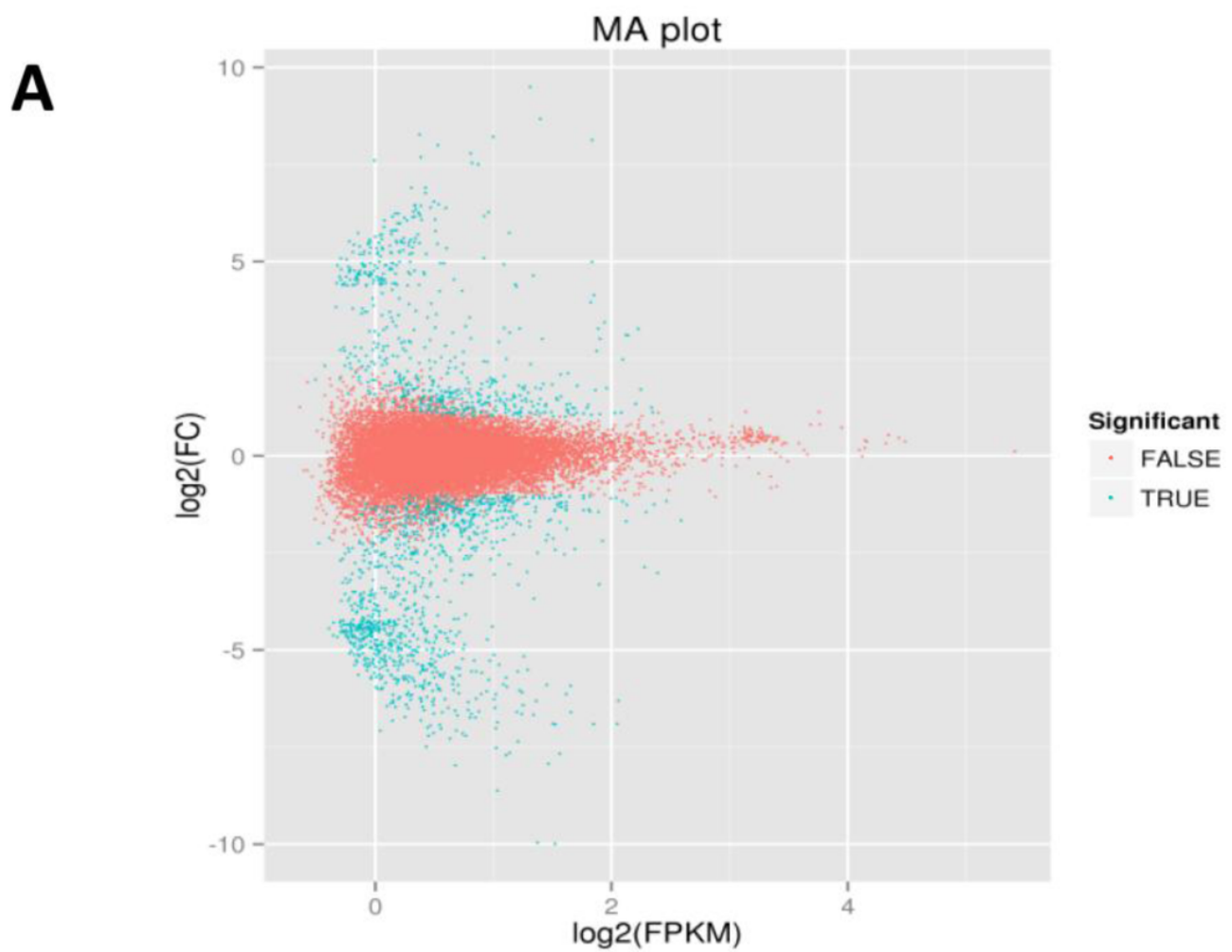
Distribution of the most common GO term categories.



# 4

The DEGs in the papilla and skin of sea cucumber.

(A) M-A plots showing gene expression in papilla and skin. The x-axis represents the logarithm of FPKM and y-axis represents the logarithm of foldchange; (B) Venn diagram displays the number of papilla-specific, skin-specific, and co-expressed genes.



## 5

Comparison between RNA-Seq results and qRT-PCR validation results.

X-axis shows genes in two tissues validated in this study; Y-axis shows Log<sub>2</sub>Ratio of expression of SK (skin) versus YZ (papilla). AAC4PL, AAC-rich mRNA clone AAC4 protein-like; Hsp26, heat shock protein 26; NP, novel protein; TN, Tenascin; EMI, EMI domain; Hp TTRE, hypothetical protein TTRE\_0000953901; FGL, Fibrinogen-like protein A; HpX975-24482, hypothetical protein X975\_24482, partial; PP2A, Serine/threonine-protein phosphatase; FIL2L, Fibrinogen-like protein A; Col- $\alpha$  FiCollagen gen-like protein A; Col-I-ase; FIL2L, Fibrinogen-like proteiphosphatealdolase; IN, Integrin alpha 2; MAD2A, Mitotic spindle assembly checkpoint protein.

